JOURNAL OF SPACECRAFT AND ROCKETS
Vol. 59, No. 4, July–August 2022

Engineering Notes

Using Plasma-Induced X-Ray Emission to Estimate Electrostatic Potentials on Nearby Space Objects

Kieran Wilson,* Julian Hammerl,* and Hanspeter Schaub†
University of Colorado Boulder, Boulder, Colorado 80301

https://doi.org/10.2514/1.A35161

I. Introduction

SPACECRAFT operating in high Earth orbit experience electrostatic charging due to interactions with the space environment. This accumulation of charge becomes hazardous under certain conditions, particularly in close-proximity and docking operations [1]. An example of such a scenario can occur during rendezvous of the Orion crew module with NASA's planned Lunar Gateway, when the Orion capsule will be shadowed by Gateway during the terminal rendezvous phase. Reference [2] shows that the change in photoelectric current could result in potential differences of several kilovolts between the two bodies, posing electrostatic discharge risks at contact. The ability to measure the relative potentials between objects, or the change in potential of the Orion module as it moves into eclipse, could help indicate the presence of hazardous potential differences.

The goal of this work is to determine the electrostatic potential on a co-orbiting object without making physical contact, i.e., touchlessly. Previous work utilized an active electron beam to excite x-rays, and examined the resulting bremsstrahlung energy spectrum to estimate the potential [3]. Incident electrons lose kinetic energy through a series of interactions with the atoms in a material. The energy the electron loses at each interaction is emitted as a photon, typically in the x-ray part of the electromagnetic spectrum, and can be modeled using functions described in [4]. The x-ray spectrum from ambient space environment electrons impacting a surface provides an intriguing alternative option for doing so without requiring an active electron beam to excite x-ray emission. Such x-rays emitted by spacecraft surfaces have been observed on spacecraft operating in Earth orbit previously, including in Refs. [5,6].

As a spacecraft charges, the accumulated potential will effectively shift the landing energy of incident electrons by either accelerating them if it accumulates a positive charge, or repelling them at negative potentials. A spacecraft charged to −10 kV, for example, will repel any incident electrons with energies below 10 keV. Therefore, the electron spectrum will be shifted by 10 kV, as seen in Fig. 1, which in turn results in reduced x-ray photon fluxes. The anticipated drop in photon fluxes can be computed for any spacecraft potential, assuming a steady electron environment, which leads to the spacecraft potential versus x-ray flux curve shown in Fig. 2. Time-varying plasma conditions require recomputation of the expected x-ray flux from the target; however, this is feasible if the local plasma conditions are monitored. This change in relative x-ray flux generalizes to positive target spacecraft potentials.

This work establishes a theoretical framework for evaluating the electrostatic potential on an object using ambient electron induced x-ray fluxes. This theoretical sensing approach is then evaluated experimentally, using a broad spectrum electron gun to simulate the space plasma environment.

II. Theory of Passive Electrostatic Charge Sensing Using X-Ray Measurements

The change in emitted x-ray quantities provides a means of determining the charge state of an object without requiring spectrum-based analysis. If the servicing craft can measure the local electron population, then the potential of the target is inferred by examining the change in x-ray emission. For a case with consistent local plasma properties, a decrease in x-ray emission would indicate negative charging, while positive spacecraft potentials would be marked by increases in x-ray emission. Therefore, this method is useful in indicating changing surface potentials in cases where the plasma remains relatively constant, where spacecraft potentials are changing much more quickly than the plasma environment. Such circumstances occur naturally when a spacecraft crosses from sunlight to eclipse conditions, or in a rendezvous scenario, when the servicer eclipses the sunlight on the target. Additionally, a small x-ray detector could even be used as a proxy for an electron spectrum monitoring instrument; a significant change in x-ray flux could be used as an indicator of changing environmental conditions, which increases charging risks.

It is worth noting that the indication of charging found here (i.e., the x-ray flux decreases as a spacecraft potential increases) runs somewhat counter to the conclusions of Ref. [8] in their analysis of using x-ray fluxes as proxy indicators of charging events. However, these two analyses apply to fundamentally different scenarios: here it is assumed that the plasma conditions are near steady state, whereas the work of Ref. [8] assumes that the spacecraft are charging due to severe geomagnetic storm events. This study therefore examines high-energy bremsstrahlung emitted by the high-energy electrons (40–180 keV) associated with geomagnetic storm conditions and arcing events, but neglects the contributions of more numerous lower-energy electrons that dominate low-energy x-ray emission even in quiet conditions. Reference [8] also focuses on high-energy x-rays, whereas this work is concerned with x-ray energies approximately an order of magnitude lower. Additionally, this work focuses on quasi-steady-state DC potentials that may vary over seconds or longer, rather than detecting arcing events or other rapid potential changes.

Two components are modeled in the simulated x-ray spectrum: characteristic radiation, which is emitted when an outer shell electron relaxes to fill an inner shell vacancy and releases the corresponding energy difference as an x-ray photon, and the continuous bremsstrahlung spectrum, which occurs primarily when energetic electrons are slowed by interactions with atomic nuclei. The energy of characteristic radiation is specific to a particular electron state transition in a specific element, so it can be used to identify the source element much like auger spectroscopy. The characteristic radiation yield, i.e., the number of characteristic photons generated per incident electron with energy E_e, is approximated by [9]

Received 10 May 2021; revision received 27 January 2022; accepted for publication 6 March 2022; published online 4 April 2022.

*Graduate Research Assistant, Ann and H. J. Smead Aerospace Engineering Sciences Department. Member AIAA.
†Glenn L. Murphy Endowed Chair, Ann and H. J. Smead Aerospace Engineering Sciences Department. Fellow AIAA.

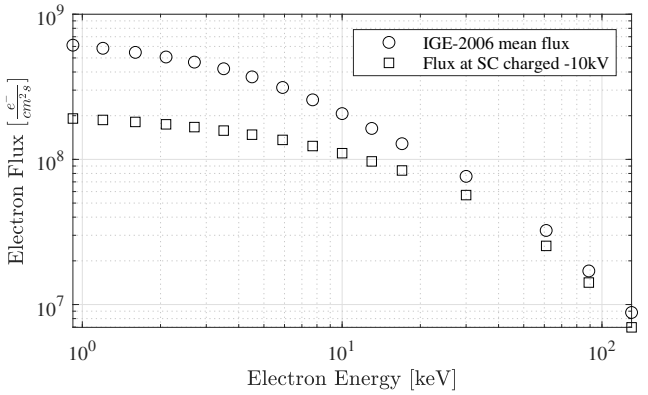

Fig. 1 IGE-2006 mean electron flux and expected electron flux observed by a spacecraft charged to −10 kV [7].

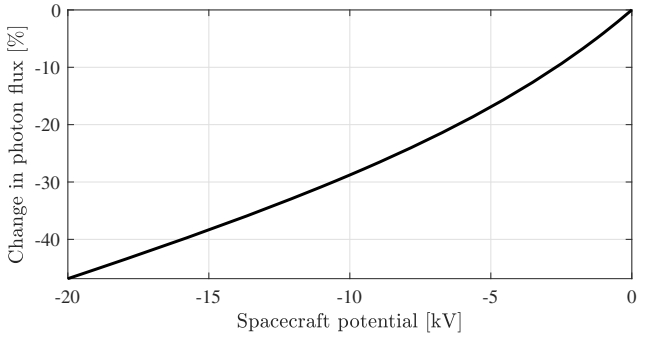

Fig. 2 Change in total x-ray photon emission due to plasma electron bremsstrahlung as a function of spacecraft potential, for a 1 m^2 aluminum plate.

$$I_p = N\left(\frac{E_e}{E_k} - 1\right)^{\alpha} \tag{1}$$

For aluminum, $N = 1.4 \times 10^{-5}$, $\alpha = 1.63$, and the characteristic emission energy $E_k = 1.49$ keV. If $E_e < E_k$, then the characteristic radiation yield is equal to zero. The number of bremsstrahlung photons with energies between E and $E + \Delta E$ generated per incident electron with energy E_0 is estimated by

$$\Delta I = C\sqrt{Z}\frac{E_o - E}{E}\left(-73.90 - 1.2446E + 36.502\ln Z + \frac{148.5E_o^{0.1293}}{Z}\right) \times \left[1 + (-0.006624 + 0.0002906E_o)\frac{Z}{E}\right]\Delta E \tag{2}$$

where Z is the atomic number of the element and C is a scaling factor that is specific to the element [10].

III. Experimental Validation of Passive Sensing

A series of experiments are carried out to validate this passive sensing method. All experiments are conducted in the ECLIPS space environment experimentation facility in Ref. [11]. The experimental setup includes three main components: a broad-spectrum electron gun aimed at a target plate, a custom-built retarding potential analyzer (RPA) to measure the electron flux, and an x-ray detector to observe the resulting x-ray spectra (Fig. 3). The 6061 aluminum target plate includes a 5 mm hole to allow the RPA, which is situated directly behind the plate, to measure the electron spectrum.

In contrast to traditional monoenergetic electron beams, the broad-spectrum electron gun of Ref. [12] emits electrons at a wide range of energies simultaneously, enabling the experimental simulation of the electron populations in the space environment. The maximum energy of the emitted spectrum corresponds to the voltage provided by a

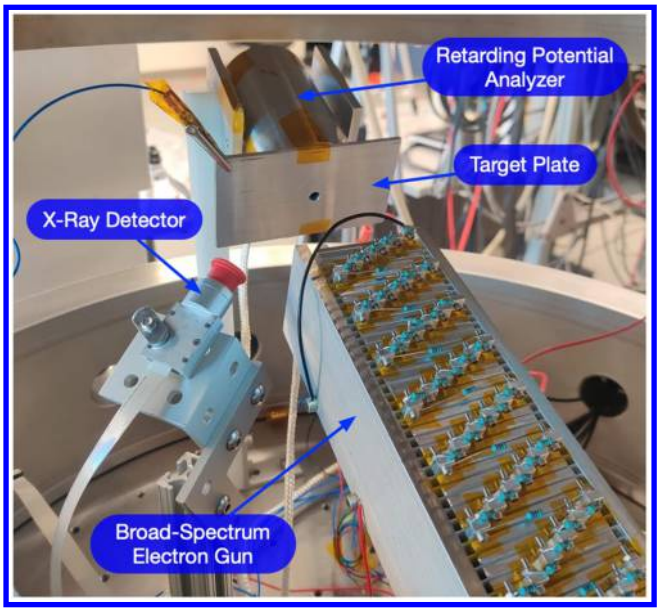

Fig. 3 Experimental setup in chamber.

power supply, a Matsusada AU series high-voltage power supply. The RPA is described in detail in Ref. [13] and consists of a grounded front grid, a discriminating grid with variable voltage, and a collection cup connected to a picoammeter. An Amptek X123 x-ray spectrometer with a 6 mm^2 Si-PIN diode sensor is used to detect the generated x-rays. The plate potential is controlled by a Spellman SL300 high-voltage power supply, and chamber pressure is kept below 1×10^{-6} Torr for all experiments. The maximum energy of the spectrum created by the broad-spectrum electron gun is set to 3.3 kV, and the observed integral electron flux for a plate potential of 0 V is shown in Fig. 4.

The experiment procedure is as follows. Before starting the electron gun, the target plate potential is set to the desired voltage. Once the electron gun is started and emits electrons onto the plate, the resulting x-ray spectra are measured by the x-ray detector, which records for 20 s such that a sufficient number of photons are detected. The RPA measures the electron flux only if the plate potential is equal to 0 V. This procedure is repeated five times for each target plate potential, and the potential on the plate is then adjusted. Plate potentials from −500 to +400 V are evaluated.

The total number of photons, I_{ph}, observed is determined for each plate potential by adding up the detected photons in every energy bin of the experimental spectrum. To obtain the change in total x-ray emission, the number of detected photons is compared to the total number of photons for a 0 V plate potential, $I_{\text{ph},0}$:

$$\Delta I_{\text{ph}} = \frac{I_{\text{ph}} - I_{\text{ph},0}}{I_{\text{ph},0}} \tag{3}$$

The theoretical change in total x-ray emission is obtained with Eqs. (1) and (2), using the mean electron spectrum of the 0 V potential tests. As described above, the electron flux is shifted for plate potentials other than 0 V to accommodate for the changing electron populations that result from a charged plate. Figure 5 shows the experimental and theoretical change in total x-ray emission for plate potentials between −500 and 400 V. The circles indicate the mean value, and the bars correspond to the 2σ interval of the five test runs for each plate potential. Figure 6 includes a histogram for the error of the estimated plate potential, i.e., the difference between the estimated potential according to the theoretical change in x-ray photons and the actual plate potential during the experiment. The errors are reasonably small, with a mean error of 23 ± 29 V 1σ, and the experimental results follow the same trend as the theoretical curve. However, there is a nonzero bias in the errors shown in Fig. 6, and the theoretical curve seen in Fig. 5 appears to overpredict the change in

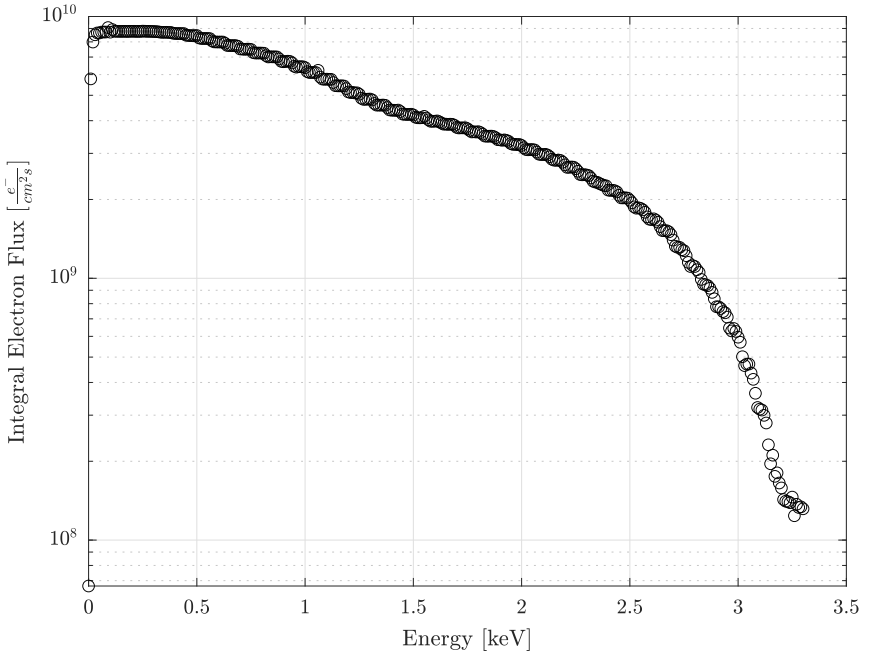

Fig. 4 Integral electron flux of the broad-spectrum electron gun up to 3.3 keV, measured by the retarding potential analyzer.

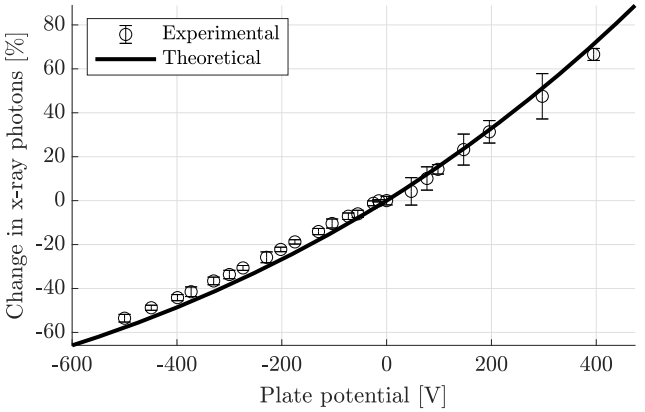

Fig. 5 Experimental change in total x-ray photon emission due to ambient plasma as a function of plate potential.

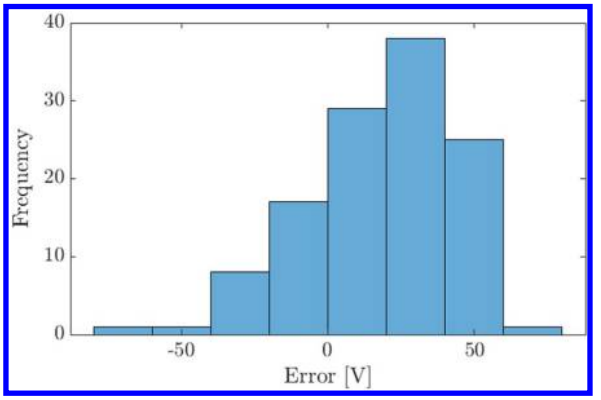

Fig. 6 Error of the estimated plate potential for data in Fig. 5.

photon flux for both positive and negative potentials. This is due to the angular distribution of bremsstrahlung radiation, which favors emission in certain directions dependent on the energy of the incident electron. The models used in this work to estimate bremsstrahlung radiation are based on an angle-integrated formulation, which does not account for these directional effects. The experiments with a monoenergetic beam in Ref. [14] show no statistically significant dependence between detector-beam separation angle and landing energy computation accuracy. However, the angles evaluated are limited to $\pm 30°$ from beam normal by the x-ray detector ribbon cable constraints. In this case the detector is positioned closer to 60° from beam normal, and beam normal is less defined due to the wide range of electron trajectories emerging from the broad spectrum electron gun. Both of these effects can lead to directional anisotropy in the resultant spectrum.

The limited accuracy of the utilized analytical expression of the bremsstrahlung model motivates alternative means of improving the passive electrostatic potential estimation method.

One way to mitigate the effects of the directional dependency of bremsstrahlung emission and the limitation of the analytical approximations is to look at only part of the x-ray spectrum, specifically the characteristic radiation. Unlike bremsstrahlung radiation, characteristic radiation is emitted isotropically, avoiding angular anisotropy concerns. The theoretical change in x-ray photons is found by using Eq. (1) to compute the expected number of emitted characteristic x-rays for a given incident electron flux. As discussed previously, characteristic radiation is emitted at a specific energy, but due to in-detector spreading effects, a Gaussian peak in the x-ray spectrum is observed.

To filter out the bremsstrahlung radiation from the experimental spectrum, a Gaussian function is fitted to the characteristic peak. The energy level where the experimental spectrum starts to deviate significantly from the Gaussian function gives information about both the width of the characteristic peak and the intensity of the bremsstrahlung radiation at that energy. The resulting number of photons corresponds approximately to the photons emitted as characteristic x-rays. Equation (3) is used for the computation of the theoretical and experimental change in characteristic x-ray photon emission, and the results are shown in Fig. 7.

The theoretical curve aligns closely with the experimental values, with the error bars encompassing the true value in every case shown in Fig. 7. Comparing the results of the characteristic photon emission to the results of total photon emission (including the bremsstrahlung radiation) suggests that using the characteristic yield alone provides a better way to passively estimate the electrostatic potential of the plate. Figure 8 shows the errors of the estimated plate potential, which are in a similar range as the errors of the landing energy estimation that utilizes an active mono-energetic electron beam [3]. The strong agreement between the theory and the experimental results

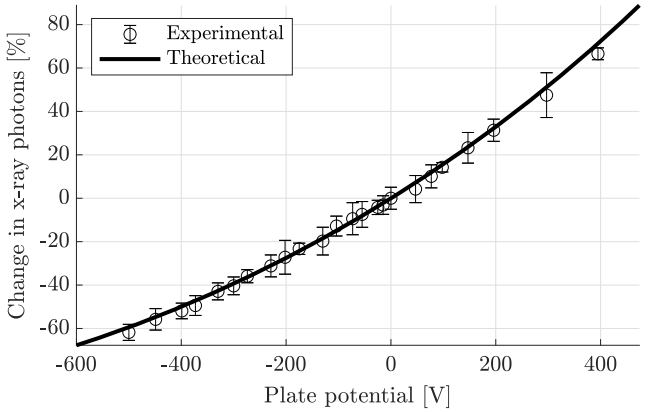

Fig. 7 Change in characteristic x-ray photon emission due to ambient plasma as a function of plate potential.

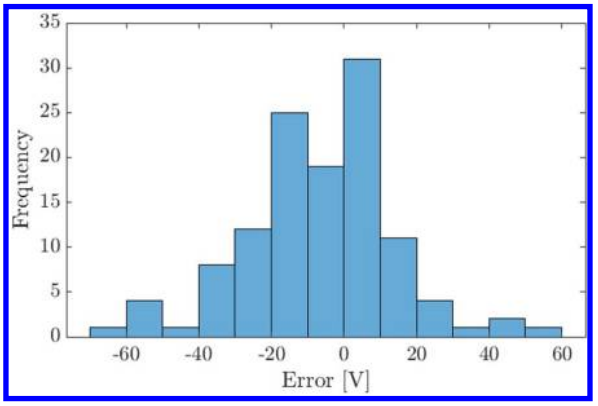

Fig. 8 Error of the estimated plate potential for the set of points shown in Fig. 7.

(just 7 ± 20 V 1σ mean error) indicate that this passive sensing method provides a promising approach of touchlessly estimating the electrostatic potential of a nearby object without using an electron beam.

IV. Conclusions

Environmentally induced x-rays provide a compelling means of electrostatic potential estimation if the environmental electron flux is known. This is demonstrated theoretically, and through experimentation using a novel electron gun design to simulate the space environment. Due to the angular dependency of bremsstrahlung radiation and the limitations of the utilized model, the accuracy of this passive sensing method can be improved by filtering out the bremsstrahlung spectrum and considering characteristic photons only. The precision of this method is comparable to the performance of the active sensing method that uses a mono-energetic electron beam.

Acknowledgment

This work was supported through Air Force Office of Scientific Research Grant #FA9550-20-1-0025.

References

[1] Lai, S. T., *Fundamentals of Spacecraft Charging: Spacecraft Interactions with Space Plasmas*, Princeton Univ. Press, Princeton, NJ, 2011, Chaps. 1, 2.

[2] Goodman, M., Paez, A., Willis, E., and DeStefano, A., "An Analytic Model for Estimating the First Contact Resistance Needed to Avoid Damaging ESD During Spacecraft Docking in GEO," *Applied Space Environments Conference*, Lunar and Planetary Inst., Universities Space Research Assoc., 2019.

[3] Wilson, K., Bengtson, M., and Schaub, H., "X-Ray Spectroscopic Determination of Electrostatic Potential and Material Composition for Spacecraft: Experimental Results," *Space Weather*, Vol. 18, No. 4, 2020, pp. 1–10.
https://doi.org/10.1029/2019SW002342

[4] Lamoureux, M., and Charles, P., "General Deconvolution of Thin-Target and Thick-Target Bremsstrahlung Spectra to Determine Electron Energy Distributions," *Radiation Physics and Chemistry*, Vol. 75, No. 10, 2006.
https://doi.org/10.1016/j.radphyschem.2006.06.006

[5] Horack, J. M., Fishman, G. J., Meegan, C. A., Wilson, R. B., and Paciesas, W. S., "BATSE Observations of Bremsstrahlung from Electron Precipitation Events," *AIP Conference Proceedings*, Vol. 265, No. 1, 1991, pp. 373–377.
https://doi.org/10.1063/1.42765

[6] Kruk, J. W., Xapsos, M. A., Armani, N., Stauffer, C., and Hirata, C. M., "Radiation-Induced Backgrounds in Astronomical Instruments: Considerations for Geosynchronous Orbit and Implications for the Design of theWFIRSTWide-Field Instrument," *Publications of the Astronomical Society of the Pacific*, Vol. 128, No. 961, 2016, Paper 035005.
https://doi.org/10.1088/1538-3873/128/961/035005

[7] Sicard-Piet, A., Bourdarie, S., Boscher, D., Friedel, R. H. W., Thomsen, M., Goka, T., Matsumoto, H., and Koshiishi, H., "A New International Geostationary Electron Model: IGE-2006, from 1 keV to 5.2 MeV," *Space Weather*, Vol. 6, No. 7, 2008.
https://doi.org/10.1029/2007SW000368

[8] Ferguson, D. C., Murray-Krezan, J., Barton, D. A., Dennison, J. R., and Gregory, S. A., "Feasibility of Detecting Spacecraft Charging and Arcing by Remote Sensing," *Journal of Spacecraft and Rockets*, Vol. 51, No. 6, 2014.
https://doi.org/10.2514/1.A32958

[9] McCall, G. H., "Calculation of X-Ray Bremsstrahlung and Characteristic Line Emission Produced by a Maxwellian Electron Distribution," *Journal of Physics D: Applied Physics*, Vol. 15, No. 5, 1982, pp. 823–831.
https://doi.org/10.1088/0022-3727/15/5/012

[10] Trincavelli, J., and Castellano, G., "The Prediction of Thick Target Electron Bremsstrahlung Spectra in the 0.25–50 keV Energy Range," *Spectrochimica Acta Part B: Atomic Spectroscopy*, Vol. 63, No. 1, 2008, pp. 1–8.
https://doi.org/10.1016/j.sab.2007.11.009

[11] Wilson, K. T. H., Bengtson, M., Maxwell, J., Calvo, A. R., and Schaub, H., "Characterization of the ECLIPS Space Environments Simulation Facility," *AIAA SciTech Conference*, AIAA, Reston, VA, 2021.

[12] Bengtson, M., Wilson, K., and Schaub, H., "Broad-Spectrum Electron Gun for Laboratory Simulation of Orbital Environments," *Proceedings of the 2021 AIAA SciTech Forum and Exposition*, AIAA, Reston, VA, 2021.

[13] Bengtson, M., "Electron Method for Touchless Electrostatic Potential Sensing of Neighboring Spacecraft," Ph.D. Thesis, Univ. of Colorado, Boulder, CO, 2020.

[14] Wilson, K., "Remote Electrostatic Potential Determination for Spacecraft Relative Motion Control," Ph.D. Thesis, Univ. of Colorado, Boulder, CO, 2021.

V. J. Lappas
Associate Editor